Cyclic behaviour of grouted duct connections in RC precast structures

Comportamento ciclico di connessioni iniettate in strutture prefabbricate in CA

Lorenzo Hofer[1], Mariano Angelo Zanini[2], Flora Faleschini[3], Klajdi Toska[4], Marco Nucci[5], Carlo Pellegrino[6]

[1,2,3,4,6] *Dept. of Civil, Environmental and Architectural Engineering, University of Padova, Padova, Italy*

[5] *NUOVA TESI SYSTEM S.r.l., Casale sul Sile, Treviso, Italy*

ABSTRACT: The paper investigates the cyclic behaviour of a column-to-foundation joint for precast concrete structures. The connection investigated in the experimental campaign is realized using corrugated steel ducts in which column protruding longitudinal rebars are anchored by grouted high performance mortar. The research program includes six full-scale RC columns having a square section, tested under an increasing cyclic lateral load and a constant axial load, with the aim to investigate the influence of the connection typology (cast-in-place or grouted connection), of different bar anchorage lengths and of different rebars diameters. Results are analysed in terms of hysteretic behaviour, energy dissipation, ductility values and plastic hinge location, and show a comparable structural behaviour between specimens with the precast joint and reference cast-in-place ones. / Questo lavoro indaga il comportamento strutturale ciclico di una particolare tipologia di giunto colonna-fondazione per strutture prefabbricate in calcestruzzo armato. La connessione analizzata nella campagna sperimentale è realizzata tramite un tubo metallico corrugato annegato nel plinto di fondazione, nel quale vengono ancorate le barre longitudinali della colonna tramite l'iniezione di malta ad alta resistenza. Nella campagna sperimentale vengono testate sei colonne di sezione quadrata in scala reale, applicando uno spostamento orizzontale ciclico crescente contemporaneamente ad uno stato costante di compressione, con l'obiettivo di valutare l'influenza dei seguenti parametri: tipologia di connessione (prefabbricata e gettata in opera), diversa lunghezza di anco-raggio, diverso diametro delle barre di armatura. I risultati sono quindi analizzati in termini di comportamento isteretico complessi-vo, dissipazione energetica, duttilità e localizzazione delle cerniere plastiche, e mostrano una risposta strutturale comparabile tra i provini con la connessione iniettata e i corrispondenti provini di riferimento gettati in opera.

KEYWORDS: column-to-foundation connection; grouted duct connection, precast concrete structures, cyclic test; seismic behaviour / connessione colonna-fondazione; connessione iniettata; strutture prefabbricate; test ciclico, comportamento sismico

1 INTRODUCTION

Reinforced concrete precast structures are widely diffused structural typologies, especially adopted to realize industrial plants, factories and warehouses (Buratti et al. 2017). Especially for this structural typology, connections play a key role since they allow the structural elements to be prefabricated and then only assembled on site. The common configuration of this kind of structures adopts cantilever columns connected with simply supported beams. Consequently, the structural behaviour of the column base highly influences the overall structural response. When precast frame structures are subject to horizontal forces, the ductility demand is concentrated at the base of the column, which becomes the most critical part of the structure. Consequently column-to-foundation connections have to ensure an overall strength, ductility and dissipation comparable with those of the common cast-in-place (CIP) connections (Negro and Toniolo 2012).

In last years, several column-to-foundation connection types have been developed and tested and can be summarized into two main typologies:

i. traditional connection, where the entire column is inserted into a pocket foundation;

ii. connections aimed to directly connect the column's longitudinal bars or the bottom of the column to the foundation.

The latter ones that can be furtherly subdivided into two groups:

iia. connections adopting bar couplers or bolted connections;

iib. connections with high performance mortar grouted in corrugated ducts.

Between the two typologies *i* and *ii*, pocket foundations represent the older solution. In this construction technique, the temporary bearing and the vertical alignment is ensured by the crane and by provisional props. Once positioned, the joint is filled with in-situ concrete pouring. Typically, such solution implies large excavations and difficult transpor-

tation. More information and extensive experimental test on this construction technique can be found in Saisi & Toniolo 1998, and Xu et al. 2021.

In recent years, scientific research mainly focused on the second connections typology, aiming to develop construction techniques able to speed up the on-site construction process. Regarding the connection type *iia*, Philippi & Hegemier (2013) adopted mechanical bar couplers for connecting the reinforcement bars at the base of the column, while Haber et al. (2012) investigated the behaviour of two other couplers, consisting of up-set headed couplers and grouted sleeve couplers. Further studies and experimental campaign can be found in Al-Jelawy et al. (2017) and Wang et al. 2021. Finally, an extensive experimental campaign aimed to investigate the structural behaviour of four different mechanical column-foundation connections devices that can be included in the *iia*, is reported in Dal Lago et al. (2016).

In the last approach *iib*, reinforcement bars protruding from one precast element are grouted into corrugated steel ducts encased in the other unit. Usually, high performance mortar is adopted. This connection type is mainly applied in column-to-column and column-to-foundation connections. For the former case, readers are referred to Zheng (1996) and Tullini & Minghini (2016); both works showed the overall good behaviour of such kind of connection. Regarding the column-to-foundation connections, two main solutions were studied in scientific literature. The first, in which bars protruding from the foundation are anchored in the column and then the opposite one, in which longitudinal rebars protruding from the column are anchored in the foundation. While the former connection was tested in several experimental campaigns (Belleri & Riva 2012; Popa et al. 2015; Tullini & Minghini 2020), the latter was little investigated. In particular, Buratti et al. 2012 tested a one column with protruding bars anchored in foundation. Although the overall response turned out to be promising and satisfying, the steel tube used to center the column, influenced the column behaviour.

In the above context, this work wants to enlarge the current knowledge on the latter type of connection in which longitudinal bars protruding from the column base are anchored in the foundation by high performance mortar grouted in corrugated steel ducts. Further details on this work can be found in Hofer et al. 2021.

2 ANCHORAGE LENGTH DETERMINATION

For estimating the anchorage length values to adopt in the full-scale columns, a preliminary experimental campaign consisting in a series of pull-out test was carried out. Two rebar diameters were adopted among those mostly adopted in precast concrete structures, i.e., 24 mm and 30 mm, respectively d_{b1} and d_{b2}. Grouted specimens were realized with both the diameter bars, whereas only 24 mm reinforcing bars were used to cast reference samples, these latter realized with reinforcing bars directly embedded in concrete. For d_{b1} grouted specimens, five anchorage lengths a_L were analysed: 10, 14, 17, 22 and 26·d_{b1}, thus varying between 240 and 624 mm, while for the reference d_{b1} specimens only three a_L values were considered (17, 22 and 26·d_{b1}). Instead, for d_{b2}, only grouted specimens were considered with only the three highest values of a_L (17, 22 and 26·d_{b2} corresponding to 510, 660 and 780 mm). For each configuration, three specimens were tested. Figure 1 shows a summary of the tested specimens, while Table 1 list the mechanical property of concrete (compressive cubic strength $f_{c,cube}$ and tensile strength f_t) and mortar (compressive cubic strength $f_{c,cube}$ and flexural strength f_f evaluated on 40 × 40 × 160 mm prism according to EN 1015 series) at the day of the test. According to the Italian Code for Construction (NTC 2018), C25/30 concrete strength class and B450C steel class are adopted.

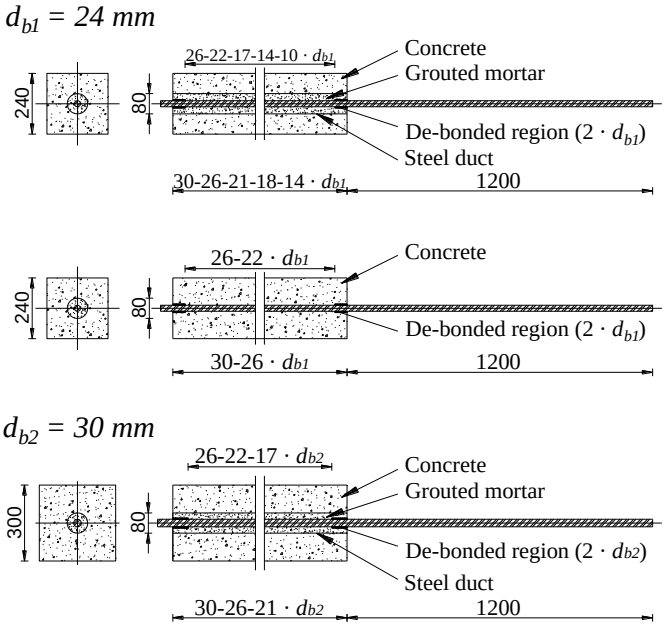

Figure 1. Geometry of the pull-out specimens / Geometria dei provini di pull-out.

Table 1. Mechanical property of concrete and mortar adopted in the pull-out specimens / Proprietà meccaniche del calcestruzzo e della malta utilizzati nei provini di pull-out.

Connection Type	a_L	Concrete		Mortar	
		$f_{c,cube}$	f_t	$f_{c,cube}$	f_f
		MPa	MPa	MPa	MPa
Grouted	10·d_{b1}	40.1	4.08	73.8	7.41
Grouted	14 and 17·d_{b1}	50.8	3.44	86.1	7.15
Grouted	22 and 26·d_{b1}	44.2	4.16	83.1	7.55
Reference	22 and 26·d_{b1}	42.3	3.83	-	-
Grouted	17,22 and 26·d_{b2}	50.3	4.28	63.7	7.16

Lastly, the corrugated ducts adopted are typical post-tensioning ducts, made with corrugated galvanized strip steel with an 80 mm internal diameter, an 84

mm external diameter, and a 0.6 mm thickness. Figure 2a shows the test layout, consisting of the concrete specimen located over the moving head of the universal machine with the steel bar gripped by two steel jaws. The load was applied by lifting the upper moving head at a velocity of 1.5 mm/min. Finally, at the top of the specimen, on the unloaded protruding bar, a 25 mm linear-variable displacement transducer (LVDT) was placed for recording the relative slip between concrete and the bar. Results shows that in the grouted duct specimens with an embedment length between $26 \cdot d_b$ and $17 \cdot d_b$, tensile failure of the steel bar occurred, for both the investigated diameters d_{b1} and d_{b2} (Fig. 2b). Specimens with anchorage length of $14 \cdot d_{b1}$ and $10 \cdot d_{b1}$ showed a satisfying response too, characterized by the bar yielding, but in some cases the splitting failure of the concrete cover occurred before the bar tensile failure (Fig. 2c). On the contrary, in the specimens where bars were directly immersed in concrete, even the highest anchorage length of $26 \cdot d_{b1}$ was not enough for ensuring the bar failure in all the three specimens (Fig. 2d). Results are summarized in Table 2.

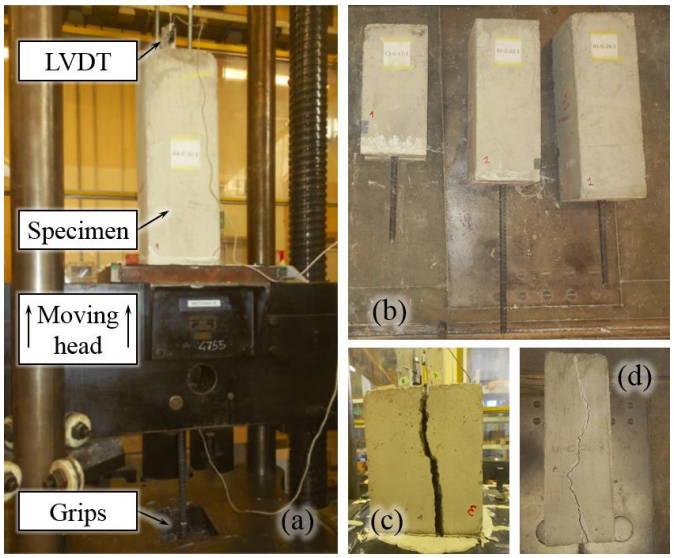

Figure 2. Pull-out test setup (a); bar fracture for specimens with a_L between $26 \cdot d_b$ and $17 \cdot d_b$ (b); splitting failure for specimens with a_L of $10 \cdot d_{b1}$ and $14 \cdot d_{b1}$ (c); splitting failure for reference specimens (d) / Setup delle prove di pull-out (a); rottura della barra per provini con a_L compresa tra $26 \cdot d_b$ and $17 \cdot d_b$ (b); rottura per splitting in provini con a_L di $10 \cdot d_{b1}$ and $14 \cdot d_{b1}$ (c); rottura per splitting nei provini di riferimento in calcestruzzo (d).

In all cases where the bar failure was reached, there was no visible damage on the grouted mortar and the slip values at the unloaded end were in the order of 10^{-2} mm. This preliminary experimental campaign showed that the grouted duct solution is able to provide a satisfying bar anchorage, higher than the one of the reference specimens, even at low embedment length values. According to the above results, the anchorage length of $26 \cdot d_b$ and $17 \cdot d_b$ were selected for anchoring the longitudinal bar of the full-scale RC columns.

Table 2. Results of pull-out test (BF = bar failure, SY = splitting failure with bar yielding, S = splitting failure without bar yielding) / Risultati dei test di pull-out (BF = rottura della barra, SY = rottura per splitting con barra snervata, S = rottura per splitting con barra elastica).

Grouted duct			
d_{b1} = 24 mm		d_{b2} = 30 mm	
a_L	Failure mode	a_L	Failure mode
$26 \cdot d_{b1}$	3 BF	$26 \cdot d_{b2}$	3 BF
$22 \cdot d_{b1}$	3 BF	$22 \cdot d_{b2}$	3 BF
$17 \cdot d_{b1}$	3 BF	$17 \cdot d_{b2}$	3 BF
$14 \cdot d_{b1}$	2 BF + 1 SY	-	-
$10 \cdot d_{b1}$	1 BF + 2 SY	-	-
Reference only concrete specimens			
$26 \cdot d_{b1}$	2 BF + 1 SY		
$22 \cdot d_{b1}$	1 BF + 1 SY + 1 S		

3 EXPERIMENTAL CAMPAIGN

The experimental campaign presented in this work includes six full-scale RC columns, having a square section and tested under a combined cyclic horizontal load and a constant compressive axial load. The parameters investigated are:

- connection type (cast-in-place or grouted, respectively indicated as CIP and G);
- bar diameter (d_{b1} = 24 mm and d_{b2} = 30 mm);
- anchorage length ($a_{L1} = 26 \cdot d_b$ and $a_{L2} = 17 \cdot d_b$, respectively indicated as *F* for the full anchorage length and *R* for the reduced one).

3.1 *Specimen geometry*

The columns tested in this experimental campaign have a square section of 400 mm side and 2900 mm height, while the foundations footprint is in all cases of 1400 × 1800 mm. Two different foundation hights of 700 mm and 850 mm are adopted for ensuring the anchorage length of $26 \cdot d_{b1}$ and $26 \cdot d_{b2}$ respectively for the column with 24 and 30 mm protruding rebars. Figure 3a shows the details of longitudinal and transverse reinforcement of the six columns, while Figure 3b show the lateral view of the investigated specimens. A summary of each column reinforcement details is reported in Table 3. Note that stirrups have a 100 mm spacing at the column base, and 150 mm in the upper part.

Table 3. Longitudinal reinforcement and stirrups details / Dettagli dell'armatura longitudinale e delle staffe.

Specimen	Longitudinal reinforcement	Stirrups		Anchorage length - a_L	
		Bars	Spacing		
		-	mm	mm	d_b
G-24-F	4 Φ 24 +4 Φ 12	Φ10	100/150	624	26
G-24-R				408	17
CIP-24				-	-
G-30-F	4 Φ 30 + 4 Φ 12			780	26
G-30-R				510	17
CIP-30				-	-

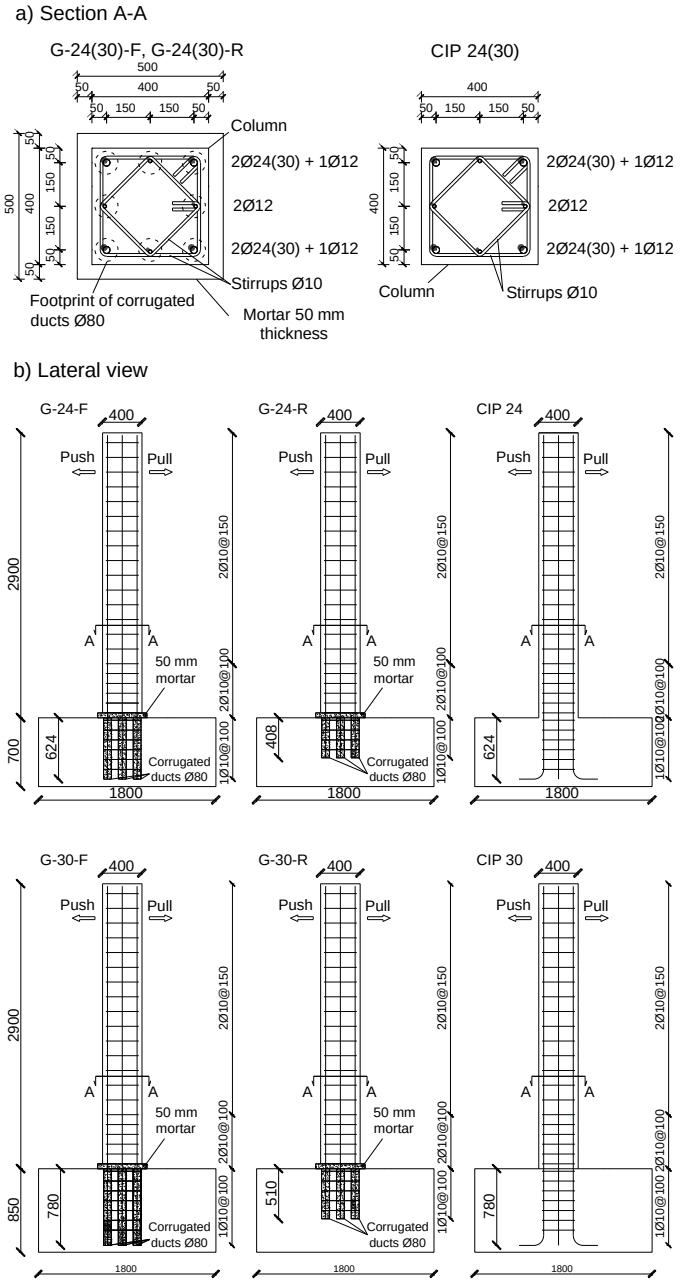

Figure 3. Reinforcement details (a) and lateral view (b) of the six columns (dimension in mm) / Dettagli di armatura (a) e vista laterale (b) delle sei colonne (dimensioni in mm).

3.2 *Material and fabrication*

Two different concrete classes were adopted for columns and foundations, respectively C45/55 and C25/30. The choice of adopting two strength classes is owned to the current engineering practice, where foundations have typically a reduced strength class (unless for peculiar durability issues) than elevation structures, and particularly, less than precast elements. For each element, a single concrete batch was realized for the column and one for the foundation: concrete properties are listed in Table 4 in terms of compressive strength at the time of specimen testing (≈40 days, $f_{c40,cube}$), tensile strength via the Brazilian test (f_t) and the secant modulus of elasticity (E_c). According to NTC 2018, reinforcement bars were realized with B450C steel: Table 5 shows the steel property in terms of average yield strength f_y, average ultimate tensile strength f_u and average percentage elongation at maximum force ε_t. Finally, the grouted mortar has, at the day of the test, a cubic compressive strength of 63.2 MPa and a flexural strength evaluated on 40 × 40 × 160 mm prism of 9.4 MPa.

Table 4. Properties of hardened concrete / Proprietà del calcestruzzo indurito.

Specimen	Column			Foundation		
	$f_{c40,cube}$	f_t	E_c	$f_{c40,cube}$	f_t	E_c
	MPa	MPa	GPa	MPa	MPa	GPa
G-24-F	71.4	4.4	42.0	50.6	4.1	34.1
G-24-R	67.5	4.1	41.5	60.5	4.5	37.1
CIP-24	62.3	5.5	38.2	63.8	5.5	39.8
G-30-F	73.5	4.2	40.2	57	5.6	37.4
G-30-R	78.0	5.1	39.4	60.6	4.4	35.6
CIP-30	60.5	4.4	36.7	60.5	4.9	38.0

Table 5. Properties of reinforcing steel / Proprietà dell'acciaio di armatura.

Bar diameter	f_y	f_t	ε_t
mm	MPa	MPa	%
10	526	623	12.0
24	537	648	17.4
30	572	673	19.8

Finally, Figure 4 shows some photos of the realization process. First the foundation was realized with the eight embedded corrugated ducts (Fig. 4a), together with the column with the protruding longitudinal bars (Fig. 4b). Figure 4c, d show how the connection is completed through the addition of the high-performance mortar: first, some small steel plates are used to space the column from the foundation, and at the same time allowing the mortar to seal the connection without any voids, the mortar is injected.

Figure 4. Realization of the grouted connections / Realizzazione delle connessioni iniettate.

3.3 *Test setup*

As Figure 5 shows, a cantilever scheme was adopted for testing the columns. The lateral displacement was applied at the top of the column by a hydraulic horizontal actuator, while the axial load was applied at the top of the column by a hydraulic jack that allows to tension two tie roads hinged at the base of the column, thus inducing a compression in the column. The axial load was kept constant for all the testing time. For the set of columns reinforced with d_{b1} bars, a compressive load of 350 kN was kept constant during the test, while an axial force of 300 kN was adopted for specimens with d_{b2} longitudinal rebars. Tests were performed by imposing a horizontal displacement in a quasi-static way, with a lateral loading rate varying from 0.1 mm/s for the lowest displacements cycles, to 0.8 mm/s for the largest ones. The test sequence was designed following the ACI 374.1-05 recommendations (ACI, 2014).

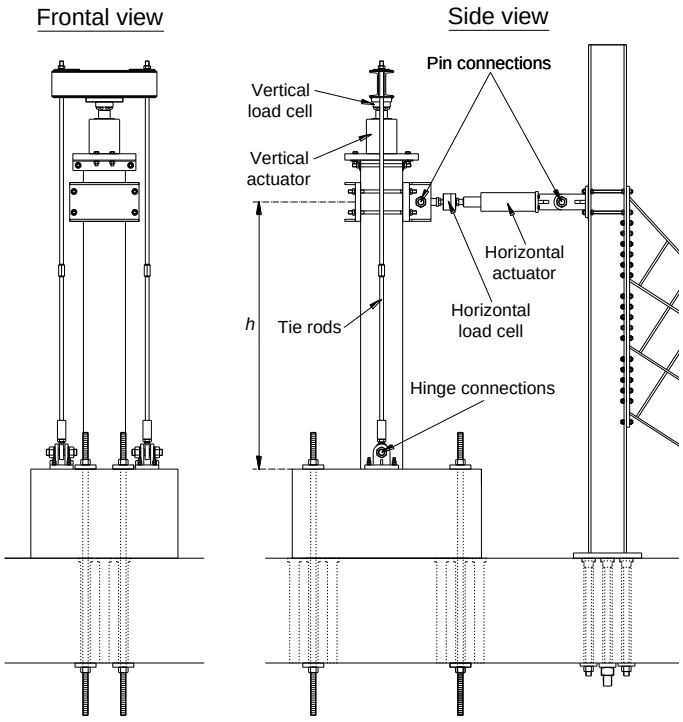

Figure 5. Test setup / Schema di prova.

Figure 6 shows the imposed displacement history in terms of drift ratio δ, defined as the ratio between the imposed top displacement Δ and the column span h, equal to 2500 mm for columns reinforced with d_{b1} = 24 mm bars, and 2550 for columns with d_{b2}. The maximum imposed drift was 5.5 and 5 %, respectively for d_{b1} and d_{b2} columns. As Figure 7 shows, in the test the following instruments were adopted:

- four LVDTs (L1-L4) and 12 linear potentiometer sensors (P1-P12) at the base of the column for measuring the column curvature;
- three wiretransducer (W1-W3) for capturing the global behaviour of the column;

four LVDTs (L5-L10) for monitoring a potential movement of the foundation.

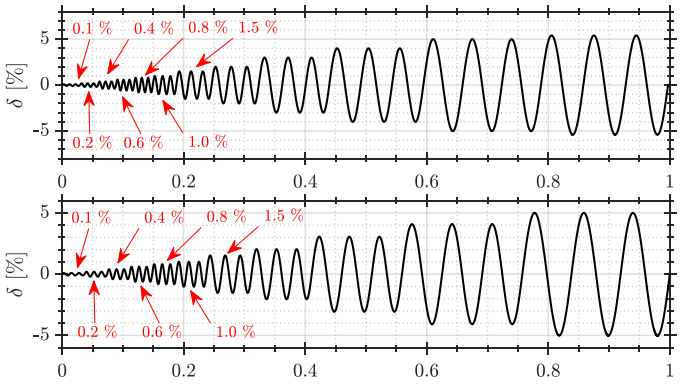

Figure 6. Lateral imposed displacement/ Spostamento laterale imposto.

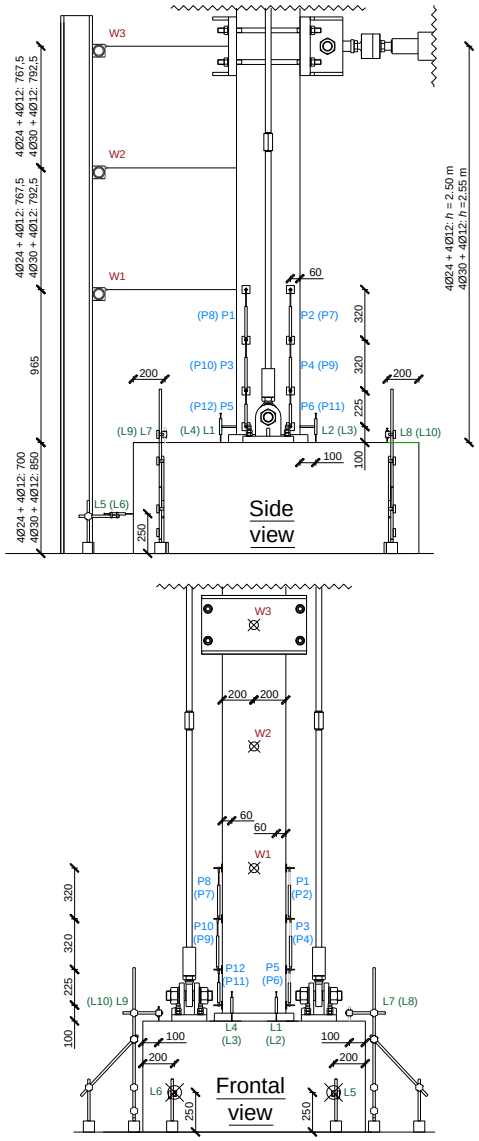

Figure 7. Measuring instrumentation/ Strumentazione di misura adottata.

4 RESULTS AND DISCUSSION

Results are herein discussed in different terms, i.e., cracking pattern, hysteresis curve, energy dissipation and plastic hinge localization.

4.1 *Cracking pattern and hysteresis curve*

All the six columns showed a similar cracking pattern, characterized by the typical horizontal cracks of the flexural failure. At the lowest drift value (δ = 0.1 %), columns behave elastically, with no cracks

occurrence. Cracks developed starting from δ = 0.2 % and gradually increased along the height of the column. At δ = 1.5 % the reinforcing bars started yielding and only few new cracks appeared, whereas the existing ones grew. From δ = 2.0 %, damage mainly increased and concentrated at the base of column (i.e., 100÷150 mm from the bottom). Figure 8 shows the damage on the columns at the end of the test. In the grouted specimens the mortar collar crushed in analogy to the CIP specimens.

Figure 8. Damage extension / Estensione del danneggiamento.

In any grouted column no macro-damage was visible in the connections. Furthermore, the intermediate longitudinal bar Φ12 in one side of column cross-section of specimen G-24-R and CIP-24, broke during the last drift level. The damage extension was totally comparable for the two series of specimens, the first with d_{b1} and the second with d_{b2}. Figure 9a and Figure 9b show the load F vs drift δ curve respectively for the d_{b1} and d_{b2} specimens.

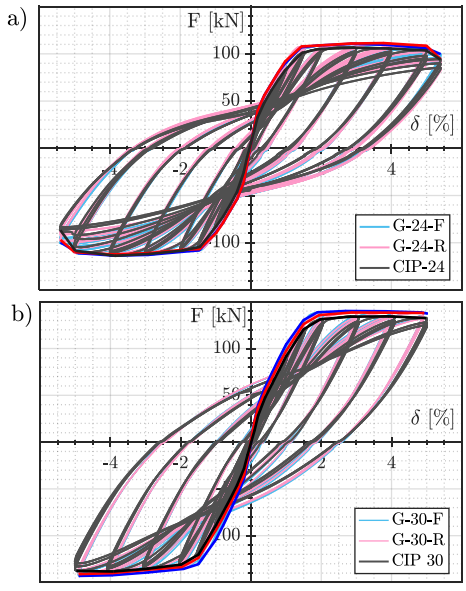

Figure 9. Load F vs drift δ curve for the specimens with d_{b1} (a) and d_{b2} (b)/ Curve carico F vs drift δ per provini con d_{b1} (a) e d_{b2} (b).

For the specimens with d_{b1} rebars, both analysing the load-drift curves and the relevant points (cracks opening, yielding and ultimate load), it is possible to state that the overall structural behaviour is comparable. They display almost symmetric behaviour in the push and pull conditions and are almost overlapping. Similar considerations can be made for columns reinforced with d_{b2} longitudinal bars. Compared to previous samples, they display slightly larger unsymmetric results. However, overall, the behaviour is considered sufficiently symmetric.

4.2 *Energy dissipation*

Measurement of the dissipated energy is a meaningful index, independently from the ductility of a structural system (Germano et al. 2016). In this section, the energy dissipation capacity is computed for evaluating the capacity of the columns to absorb energy during the entire loading history. For each i^{th} cycle, the dissipated energy $E_{d,i}$ can be computed as:

$$E_{d,i} = \iint F(\Delta)\, d\Delta \tag{1}$$

Figure 10a and Figure 10b show the dissipated energy specimens with d_{b1} and d_{b2} rebars, respectively, where both the dissipated energy for each i^{th} cycle computed according to Eq. (1). Figure 10 shows that most of the energy dissipation is concentrated at the end of the test, when the bars exceed the yielding point. For both specimens with d_{b1} and d_{b2} rebars the energy dissipation was stable for every repetition of each drift level, thus evidencing a good energy dissipation capacity. Even in terms of dissipated energy the grouted specimens behave similarly to the cast-in-places ones, for both the considered diameters d_{b1} and d_{b2}.

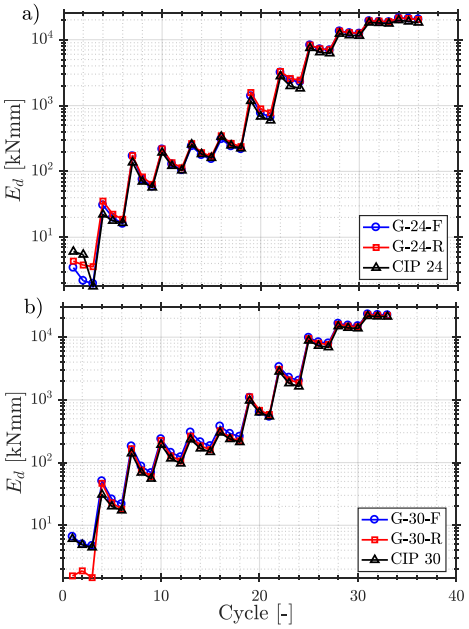

Figure 9. Dissipated energy for specimens with d_{b1} (a) and d_{b2} (b)/ Energia dissipata per provini con d_{b1} (a) e d_{b2} (b).

4.3 *Plastic hinge localization*

Finally, columns are compared also in terms of plastic hinge localization, since the plastic hinge length is an important parameter to numerically simulate the nonlinear seismic response of the structural system. According to Priestley and Park (1987), the schematic curvature distribution along a RC member at ultimate stag can be assumed as in Figure 11.

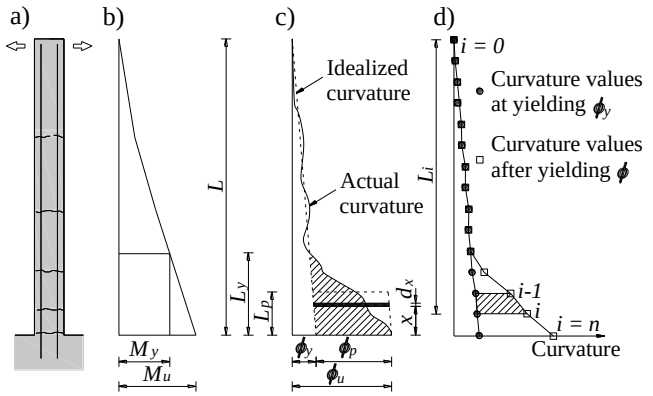

Figure 11. Schematic curvature distribution along a RC column: cracks distribution (a), bending moment diagram (b), curvature diagram (c) and model for L_p computation (d) / Andamento schematico della curvatura in una colonna in CA: stato fessurativo (a), diagramma di momento (b), andamento curvature (c), modello per il calcolo di L_p.

This distribution is composed by the yield curvature (φ_p) linearly distributed along the column height and the rectangular plastic curvature (φ_y), concentrated in the plastic zone. Typically, in the initial stages, ($M < M_{cr}$), the response is elastic and linear. For higher load levels, longitudinal bars begin to yield (φ_y and M_y, Fig. 11b), followed by concrete crushing (φ_u and M_u). Beyond the yield limit, a large increase of curvature commonly occurs at the base of the column. According to Fig. 11c, the total rotation can be subdivided into elastic (ϑ_e) and plastic (ϑ_p) rotations. In practical applications, it is convenient to refer to an equivalent plastic hinge L_p , derived by computing ϑ_p as the rectangular area $\varphi_p \cdot L_p$. For computational purposes, the equivalent plastic hinge L_p can be computed as (Jiang and Wu 2015):

$$L_p = 2L - 2\frac{\sum_{i=1}^{n} \Delta\theta_{pi} \frac{L_i + L_{i-1}}{2}}{\sum_{i=1}^{n} \Delta\theta_{pi}} \quad (2)$$

where $\Delta\theta_{pi}$ is the shaded area from section i-1 to section i. Plastic hinge lengths computed with Eq. (2) are compared with the one proposed by the Eurocode 8 (EC8), Eq. (A.9), developed for members with detailing for earthquake resistance and without lapping of longitudinal bars in the vicinity of the section where yielding is expected:

$$L_p = \frac{L_v}{30} + 0.20h + 0.11\frac{d_{bL} f_y}{\sqrt{f_c}} \quad (3)$$

Figure 12 shows for both specimens with d_{b1} and d_{b2} there are no significant discrepancies among the specimens with full and reduced anchorage lengths. Furthermore, the plastic hinge length computed with Eq. (3) well predicts the obtained values. For both rebars diameters, L_p of the cast-in-place specimens is slightly shorter than the one of the precast specimens, maybe due to the stiff restrain introduced by the small steel plates. However, this difference seems to be negligible and not influencing the overall structural behaviour of the tested connections.

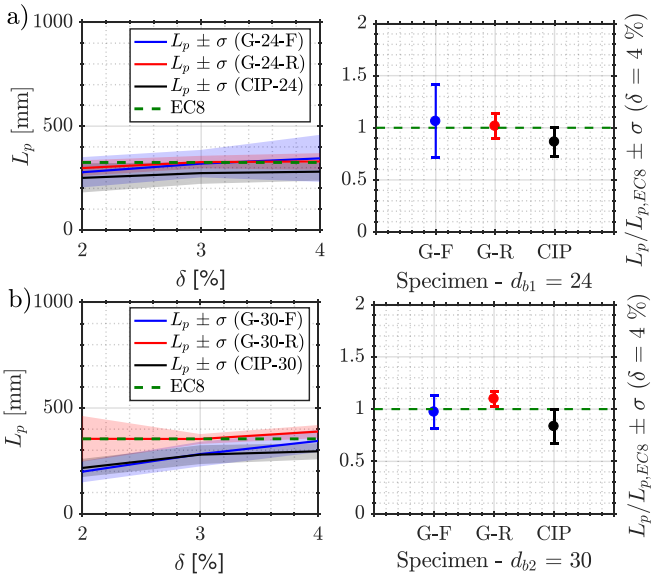

Figure 12. Comparison of L_p for d_{b1} and d_{b2} specimens with the one computed with the EC8 furmula / Confronto tra L_p calcolata per i provini con barre d_{b1} e d_{b2} e quella calcolata con la formula dell'EC8.

5 CONCLUSIONI

This paper presented the experimental campaigned aimed at investigating the structural performance of column-to-foundations connections realized with longitudinal protruding bars anchored in the foundation with high performance mortar grouted. This connection type seemed particularly efficient, since the steel ducts are well confined by the massive concrete cast of the foundation. Compared to similar technologies, this connection type avoids some specific detailing that are typical of other precast connection technologies (e.g. bar couplers, bolted and/or welded connections, detailing for confinement). According to the experimental evidences obtained in this work, it is possible to draw the following conclusions:

- a good performance of the connection was observed for all the grouted specimens with stable and symmetric hysteretic cycles. The cast-in-place and precast specimens' behaviours were comparable also in terms of ductility, dissipated energy and curvature profile;
- all the specimens exhibited a ductile flexural failure, with the formation of the plastic hinge at the base of the column. In the grouted specimens, mortar crushing occurred al the last drift levels, but no macro-damage was visible in the grouted connections.
- the two anchorage lengths adopted in this study seem sufficient to anchor the column longitudinal rebars into the foundation and to ensure a good cyclic behaviour. However, further studies are needed for investigating the joint seismic over-

strength, even considering other failure modes and in presence of significant P-Δ effects.
- The plastic hinge length was evaluated, and its value was compared with that proposed by the Eurocode 8 formulation, showing a maximum discrepancy of about 16 %.

Questo paper presenta i risultati di una campagna sperimentale volta ad indagare il comportamento strutturale di connessioni colonna-fondazione realizzate tramite ancoraggio delle barre di armatura longitudinali nel plinto di fondazione con malta ad alte prestazioni. Questo tipo di connessione sembra particolarmente efficace dato l'alto livello di confinamento costituito dal plinto. Tale connessione evita inoltre l'utilizzo di altri dispositivi, come accoppiatori meccanici, connessioni saldate o bullonate o dettagli di armatura complicati. A partire dai risultati sperimentali si possono pertanto trarre le seguenti conclusioni:
- tutti i provini con il collegamento iniettato hanno evidenziato un buon comportamento strutturale, con cicli isteretici stabili e simmetrici. I provini realizzati in opera e prefabbricati hanno dimostrato un comportamento comparabili anche in termini di duttilità, energia dissipata e profilo di curvatura.
- tutti i provini hanno avuto una rottura a flessione, con la formazione di una cerniera plastica alla base. Nei cicli finali dei provini iniettati si è assistito alla rottura del colletto di malta, senza tuttavia osservare danneggiamenti nel collegamento iniettato;
- le lunghezze di ancoraggio analizzate in questo studio si sono rivelate sufficienti a garantire un buon ancoraggio e un buon comportamento ciclico. Ulteriori studi sono necessari per investigare la sovra-resistenza sismica del collegamento, anche in presenza di un effetto P-Δ significativo;
- I valori delle cerniere plastiche calcolato sono comparabili con quelli predetti dall'EC8, con una discrepanza massima del 16%.

RINGRAZIAMENTI

The present work discusses the experimental behavior of the column-to-foundation connection of the precast system developed by NUOVA TESI SYSTEM S.r.l. who realized the tested specimens and is gratefully thanked. The authors would like also to thank Eng. Giovanni Gobbi and Eng. Enrico Rovizzi.

REFERENCES

ACI 374.1-05 (2014) Acceptance criteria for moment frames based on structural testing and commentary.

Al-Jelawy, H., Haber, Z., Mackie, K. (2017) Grouted splice precast column connections with shifted plastic hinging. In: *16th World conference on earthquake - 16WCEE 2017*, January 9-13, Santiago Chile.

Buratti, N., Bacci, L., Mazzotti, L. (2012) Seismic behaviour of grouted sleeve connections between foundations and precast columns, *in: 15th World conference of earthquake engineering (WCEE)*, 24-28 September 2012, Lisbon, Portugal, paper no. 1525.

Buratti, N., Minghini, F., Ongaretto, E., Savoia, M., Tullini, N. (2017) Empirical seismic fragility for the precast RC industrial buildings damaged by the 2012 Emilia (Italy) earthquakes. *Earthquake Engineering & Structural Dynamics*, 46: 2317 – 2335.

Belleri, A., Riva, P. (2012) Seismic performance and retrofit of precast concrete grouted sleeve connections, Precast/Prestressed Concrete Institute Journal, 57(1): 97-109.

Dal Lago, B., Toniolo, G., Lamperti Tornaghi, M. (2016) Influence of different mechanical column-foundation connection devices on the seismic behaviour of precast structures. *Bulletin of Earthquake Engineering*, 14: 3485-3508.

EN 1015-11:2019 (2019) Methods of test for mortar for masonry. Determination of flexural and compressive strength of hardened mortar.

Germano, F., Tiberti, G., Plizzari, G. (2016) Experimental behavior of SFRC columns under uniaxial and biaxial cyclic loads, *Compos B*, 85:76–92

Haber, Z.B., Saiidi, M.S., Sanders, D.H. (2012) Seismic performance of precast columns with mechanically spliced column-footing connections. *ACI Structural Journal*, 111(3): 639-650.

Hofer, L., Zanini, M.A., Faleschini, F-. Toska, K., Pellegrino, C. (2021) Seismic behavior of precast reinforced concrete column-to-foundation grouted duct connections, *Bulletin of Earthquake Engineering*, 19: 5191-5218.

Jiang, C., Wu, Y.F. (2015) Variation of plastic hinge length for RC column. In: Proceedings of the The 12th International symposium on fiber reinforced polymers for reinforced concrete structures (FRPRCS-12) & The 5th Asia-Pacific Conference on Fiber Reinforced Polymers in Structures (APFIS-2015), Joint Conference, 14–16 December 2015, Nanjing, China

Negro, P., Toniolo, G. (2012) Design guidelines for connections of precast structures under seismic actions. *EUR - Scientific and Technical Research Reports*. JRC Publication No. JRC71599. Publications Office of the European Union.

Philippi, D.J., Hegemier, G.A. (2013) Use of mechanical couplers in concrete columns. In: *Architectural Engineering Conference 2013, Pennsylvania State College, 3-5 April 2013*, United States.

Popa, V., Papurcu, A., Cotofana, D., Pascu, R. (2015) Experimental testing on emulative connections for precast columns using grouted corrugated steel sleeves, *Bulletin of Earthquake Engineering*, 13(8): 2429-2447

Saisi, A., Toniolo, G. (1998) Precast r.c. columns under cyclic loading: an experimental programme oriented to EC8. Studies and researches, F.lli Pesenti Master school. Politecnico di Milano 19:373 – 414.

Tullini N, Minghini F (2016) Grouted sleeve connections used in precast reinforced concrete construction: experimental investigation of a column-to-column joint. Engineering Structures, 127: 784-803.

Wang, R., Ma, B., Chen, X. (2021) Seismic performance of pre-fabricated segmental bridge piers with grouted splice sleeve connections. *Engineering Structures*, 229:111668.

Xu, Y., Zeng, Z., Wang, Z., Ge, J. (2021) Experimental studies of embedment length of precast bridge pier with socket connection to pile cap. *Engineering Structures* 233:111906.

Zheng, L.X. (1996) Grouted precast concrete column connections under reversed cyclic bending and compression. *ACI Structural Journal*, 93(3): 247-256.